



GEO Québec
2015

Challenges from North to South
Des défis du Nord au Sud

Non-destructive inspection of the surface of underground structures based on the propagation of surface waves

Tremblay S.P., Karray M.

Département de génie civil – Université de Sherbrooke, Sherbrooke, Québec, Canada

Chekired M., Bessette C., Jinga L.

Hydro-Québec, Montréal, Québec, Canada

ABSTRACT

This article shows how the propagation of surface waves is affected by the presence and the state of degradation of an underground concrete structure. In previous work, the behavior of elastic waves propagating in a soil profile containing an underground concrete structure was modelled using 2-dimensional numerical models. One of the drawbacks of using 2D models to represent 3D structures is that 2D models neglect the effect that out-of-plane discontinuities may have on the propagation of elastic waves. A 2D profile is therefore not fully representative of an underground profile containing a small concrete structure compared to the size of the soil deposit surrounding it. This paper uses a 3D finite difference method implemented in FLAC3D to show how the presence of a manhole and of a discontinuity at the surface of an underground concrete structure affects the propagation of surface waves.

RÉSUMÉ

Cet article démontre comment la propagation des ondes de surface est affectée par la présence et l'état de dégradation d'une structure souterraine en béton. Lors de travaux antérieurs, le comportement des ondes de surface se propageant dans un profil de sol contenant une structure souterraine a été modélisé avec des modèles numériques en 2 dimensions. L'un des inconvénients de l'utilisation de modèles 2D pour représenter des structures 3D est que les modèles 2D négligent les effets que peuvent avoir des discontinuités dans l'un des 3 axes sur la propagation des ondes élastiques. Dans le cas d'une structure souterraine de petite dimension comparativement au dépôt de sol, le profil souterrain peut cependant contenir des discontinuités dans toutes les directions. Cette étude utilise la méthode des différences finies en 3D implémentée dans FLAC3D pour montrer comment la présence d'un trou d'homme et de discontinuités à la surface d'une structure de béton souterraine affecte la propagation des ondes de surface.

1 INTRODUCTION

Underground structures play a vital role in places where the space available at the surface of the soil is limited. As time passes, these structures degrade and must be maintained in order to remain fully functional. The planning of the maintenance of underground structures will vary depending on their state of degradation which may be difficult to evaluate due to their location. The use of non-destructive techniques (NDT) for the inspection of these structures is becoming increasingly popular due to the advantages they may offer over destructive techniques. Although several NDT's are available to estimate the location of such structures, none of them has so far shown the potential to evaluate their state of degradation without requiring a direct access to them. Among the NDT's available, those based on the propagation of surface waves such as the SASW and MASW techniques are often used to evaluate the near surface elastic properties of a given soil profile (Nazarian, 1984; Gabriel et al. 1987; Karray, 1999; Park et al. 1999)

Nowadays, surface wave surveys are often performed with an array of receivers (geophones or accelerometers) placed at a regular interval along a given line. Since surface wave techniques are often reserved for applications where the properties of the soil profile do not vary considerably along the investigated profile, studies

based on surface wave propagation are mainly based on the assumption of a 1-dimensional profile where the properties of the soil only varies in function of the depth (Schwab et Knopoff, 1972, Socco et al. 2010). Although restrictive for certain types of applications, such assumptions are necessary to perform the inversion which enables the conversion of the measured surface wave's velocities into shear wave velocities. Nevertheless, 2-dimensional profile may be estimated by matching the different 1-dimensional profiles, each obtained with a different set of receivers, inverted along the investigated line (Karray et al. 2010). Surface wave techniques have also been used to detect the presence of underground features such as voids and sharp lateral changes into the properties of a given soil profile (Socco et al. 2010).

The propagation of surface waves in 2-dimensional numerical models has also been shown to be sensitive to the state of degradation of the roof of an underground structure (Tremblay et al. 2014). Unfortunately, 2D models cannot take into account the presence of discontinuities that may occur in the third (in-plane) dimension. Since the underground structures investigated in this study (Figure 1) have finite dimensions in all directions and are linked to the surface through a cylindrical manhole, 3D models are more suitable than 2D models to simulate the propagation of elastic waves.

2 THEORETICAL BACKGROUND

Elastic waves propagating in a given medium are either body or surface waves. Rayleigh waves are a specific type of surface waves that propagate along a free surface due to the interaction between compression and shear waves. Most of their energy is contained within a depth from the surface of about one wavelength. When Rayleigh waves propagate in a vertically heterogeneous medium such as a soil deposit, these waves become dispersive meaning that their velocity and energy depend on their wavelength (and frequency). In such a medium, their propagation also becomes a multimodal phenomenon (Gabriels et al.1987). For a given mode of propagation, Rayleigh waves with longer wavelengths will penetrate deeper into the soil profile than shorter wavelengths. The dispersive nature of these waves explains their popularity for near surface investigations (Socco et al. 2010).

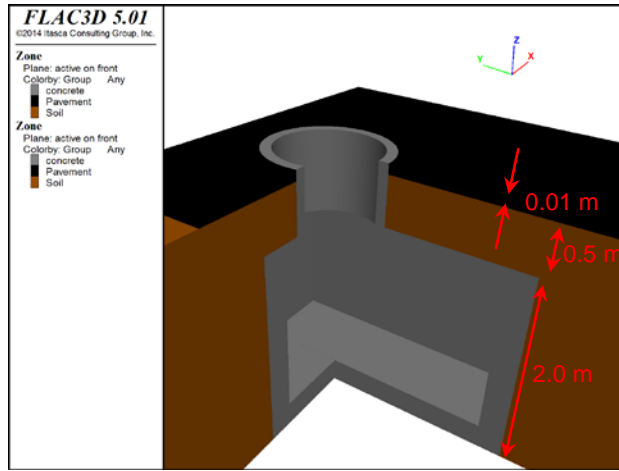


Figure 1. Side view of a cut through the X-Y axis of the 3D model. The gray zones are the concrete structure and the manhole, the brown is the soil and the black is the pavement.

In a soil profile where lateral discontinuities such as a concrete structure are present, the signals recorded by the receivers near the discontinuities will be affected by the presence of waves that were reflected or diffracted by the discontinuities (Yanovskaya, 1989; Sheu et al., 1988).

2.1 Modelling elastic waves

The homogeneous equation of motion is expressed in equation 1 for an isotropic and homogeneous continuum. Equation 1 can be solved analytically for several types of models such as an isotropic and homogeneous half space (Lamb, 1904; Aki and Richard, 2002) or for a 1 dimensional stratified media such as the ones often used in MASW (Kennet, 1979; Park et al. 1999).

$$\rho \frac{\partial^2 \mathbf{u}}{\partial t^2} = (\lambda + \mu) \nabla \nabla \cdot \mathbf{u} + \mu \nabla^2 \mathbf{u} \quad [1]$$

Where: \mathbf{u} = Displacement vector in 3D (u_x, u_y, u_z)

t = time

λ and μ = Lamé parameters

ρ = Density

$$\nabla = \left[\frac{\partial}{\partial x}, \frac{\partial}{\partial y}, \frac{\partial}{\partial z} \right]$$

However, analytical solutions are restricted to a narrow type of models making them inappropriate for a model containing strong heterogeneities. In such cases, numerical methods are used to calculate the dynamic behavior of the model. Although numerous numerical methods exist, the finite difference methods are the most popular methods for elastic wave propagation problems because of their accuracy for several class of problems, their computational efficiency and their relative ease of programming (Fichtner, 2011). In this study, the finite difference software FLAC3D was used to model the dynamic behaviors of different underground profiles.

Table 1: Elastic properties of the different materials

	Depth (m)	Bulk Modulus (Pa) $\times 10^7$	Shear Modulus (Pa) $\times 10^7$	Density (kg/m ³)
Pavement	0 to 0.1	200	100	2400
Soil	0.1 to 0.6	8.0	2.86	1900
Concrete	0.6 to 2	560	390	2500
Damaged Concrete	0.6 to 0.7	6.0	2.0	1900

3 NUMERICAL MODELS

3.1 Underground structures

The underground structures modelled in this study are similar in dimensions to the access chambers found in many cities for the transit of electricity and other utilities. These structures are typically located underneath roads or sidewalks under a shallow soil layer of less than 1 meter and are linked to the surface by a cylindrical concrete manhole. They were modelled in 3D as shown in Figure 1. The structures modelled in this study have a depth of 3 m, a length of 2 m and height 2 m while the manhole has a radius of 0.6 m and a height of 0.6 m. The elastic properties of each material are presented in table 1. The size of the models used in numerical modelling is actually larger than the size of the models shown in Figure 1. Additional zones are added to the boundaries of the models shown in Figure 1 and Figure 2 to minimize the problems of reflecting boundaries (section 3.2).

Four different models were considered in this study. All models except model 1 contain a concrete structure linked to the surface by a circular manhole. For the models 1 and 2, the structure is located under a 0.5 m deep soil layer while models 3 and 4 have a 0.1 m deep asphalt layer covering the surface of the soil. The configuration of model 4 is the same as model 3 except for the presence of a damaged zone at the surface of the roof of the concrete structure of model 4. The damaged zone is marked by dashed lines in Figure 3. Within the damaged zone, the surface of the roof of the concrete structure is uneven. The depth of the damaged zone with respect to

the original surface of the roof varies between 0 and 0.1 m.

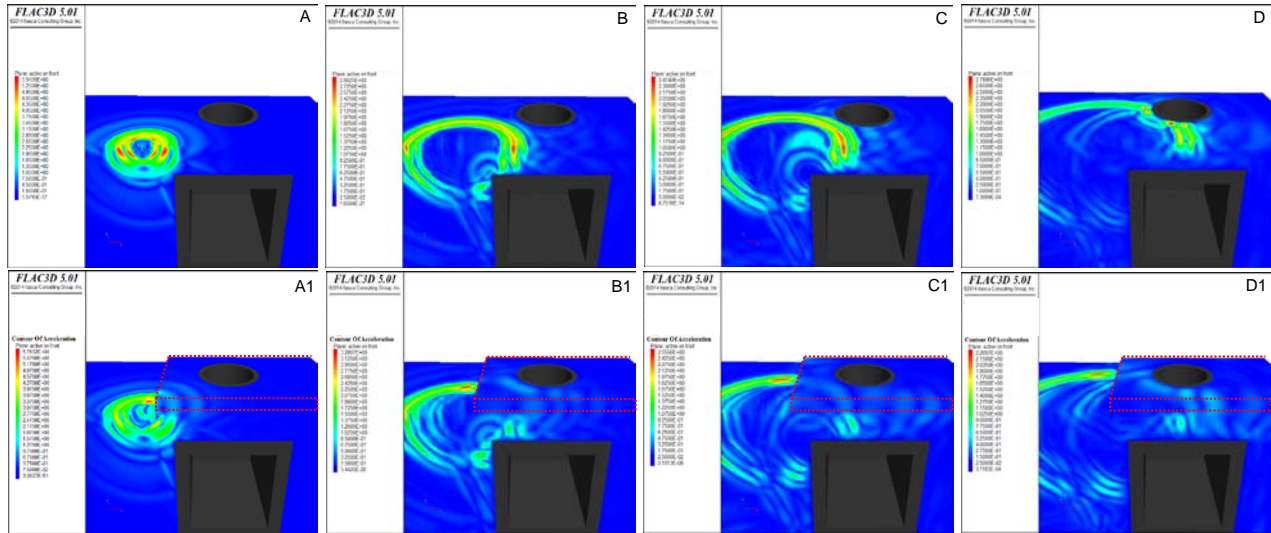


Figure 2. Contour plots of acceleration magnitude at different times for a model containing only a structure surrounded by soil (A-B-C-D) and one with a pavement at the surface of the soil (A1-B1-C1-D1). The red dotted lines indicate the location of the pavement

This zone represents the degradation of the concrete that may occur at the surface of the roof of a concrete structure as it ages.

The models 1 and 2 will be used to show how the presence of the manhole affects the propagation of surface waves. The model 3 will be used to show how the location of the receivers with respect to the position of the structure affects the recorded signals, while the model 4 will be used to show the effect of the discontinuity on the propagation of surface waves.

Table 2: Configuration of the different models (the Y means that the feature is present in the model)

		Pavement	Manhole	Damaged zone	Distance from manhole
Model 1	Line 1	N	N	N	-
Model 2	Line 2	N	Y	N	0.65 m
Model 3	Line 3	Y	Y	N	0.65 m
	Line 4	Y	Y	N	1.10 m
Model 4	Line 5	Y	Y	Y	0.65 m
	Line 6	Y	Y	Y	1.10 m

A total of 6 different lines of tests are performed over the different models as presented in table 1 and Figure 3. Figure 3 shows the location of the 6 different lines, presented as red dotted lines, with respect to the position of the structure, of the manhole and of the damaged zone which is only present for the lines 5 and 6 of model 4. In Figure 3, the upper red dotted line indicates the location of the lines 1, 2, 3 and 5 while the lines 4 and 6 are located along the lower dotted line.

3.2 Discrete grid and boundary conditions

Finite difference methods such as the one used in FLAC3D make use of a discrete grid defined by a finite

number of points distributed within the models to approximate the continuously defined wavefield (Fichtner, 2011). In order to avoid numerical distortions of the elastic waves that could occur due to the use of a discrete grid, several criteria must be respected. First, the mesh spacing must respect the following criteria (Kuhlemeyer and Lysmer 1973):

$$\Delta l \leq \frac{\lambda}{10} \quad [2]$$

Where λ is the wavelength associated with the highest frequency component that contains appreciable energy and Δl is the spatial grid element size. Since the number of elements contained within a model affects the required memory and computing time, the grid spacing is not the same throughout the entire model. The grid spacing is rather adjusted so that the finer elements are reserved only for the parts of the model that are relevant in this study. The finer elements have a depth, length and height of 0.025 m. These finer elements are reserved for the concrete elements of the roof of the structure, the soil elements located between the surface of the structure and below the pavement and for the pavement. For the other elements of the model, the grid spacing gradually increases with increasing distance from the location of the concrete structure.

Finite difference methods also require the use of an adequate time-step at which the different parameters of the model are updated. To accurately model the propagation of a given wave through the model, the time step must be adjusted in function of the faster waves propagating through the model and in function of the type of damping used. In FLAC3D, the critical or maximum time step is automatically calculated based on the properties of the model but it may also be set by the user (FLAC, 2014).

A Rayleigh damping factor with a ξ_{\min} of 2% and a ω_{\min} of 1256 rad/s was used in the present study. Quiet boundaries were used at the boundaries of the different models to minimize the amount of energy reflected by these boundaries. Quiet boundaries were shown to be an effective way to prevent the problem of reflections at the boundaries of the model without prohibiting mesh movements (Lysmer and Kuhlemeyer, 1969). The use of these boundaries alone does however not fully prevent the reflection of elastic waves. The dimensions of the models along the X-Y-Z axis should, therefore, be large enough to minimize the reflection of elastic waves at the boundaries. Finally, the models are only subjected to elastic deformations which are defined by strains lower than $10^{-3}\%$.

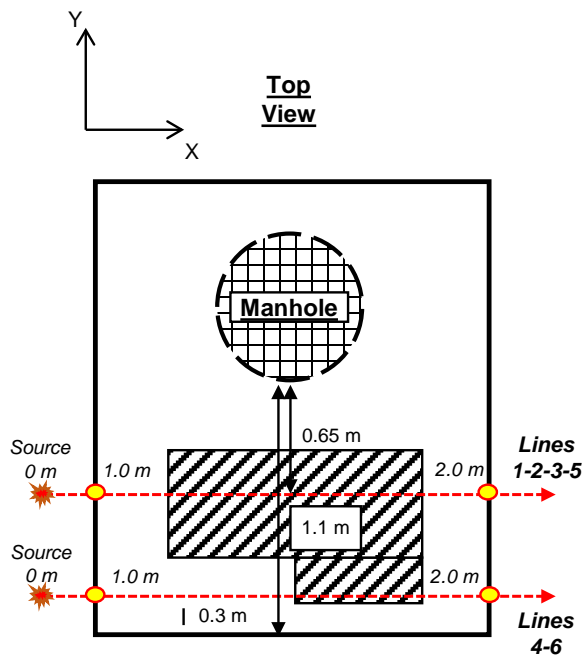


Figure 3. Top view (XY axis) of a 3D model showing the location of the damaged zone and the position of the different lines (red dotted lines) with respect to the edge of the structure and the manhole. The distances in italic characters along the red dotted lines are distances with respect to the location of the source. The position of the different lines is indicated in italic and bold characters.

3.3 Lines Configuration

The elastic waves propagating through the models are generated by the imposition of a half period sine wave at the surface of the model at a distance of 1.0 m from the position of the structure along the X-axis (Figure 3). Although the receivers can be placed directly on the pavement, the impact load, called the source, must be imposed directly at the surface of the soil (Jones, 1962; Karray and Lefebvre, 2009). The characteristics of the source were presented in Tremblay et al. 2014. The receivers are all placed along a given line as shown in Figure 3.

Although FLAC3D enables the calculation of several parameters such as the mesh displacement, velocity,

acceleration, stress, strain, etc. the only parameter that will be recorded during the simulations is the vertical acceleration measured at the surface of the models. This is to ensure that the data recorded during numerical modelling are representative of the ones obtained during a real field test where the type of accelerometer used is specifically designed to measure changes in vertical acceleration. Therefore, only the vertical acceleration measured at a regular interval of 0.1 m along the 6 different lines will be considered in this study.

4 ELASTIC WAVES PROPAGATION

As elastic waves propagate through the numerical models, their velocity and energy vary depending upon the elastic properties of the materials that they encounter. Figure 2 shows the contours of the magnitude of the total acceleration at different times across a section of 2 different models. In Figure 2, the contours A-B-C-D show the magnitude of the acceleration of a model containing only a concrete structure surrounded by soil while in A1-B1-C1-D1 a 0.1 m thick asphalt layer is placed on top of the soil layer. In the case where no pavement is present, the energy of the waves tends to remain near the surface of the soil. However, the presence of the pavement, which damps part of the frequencies propagating through the soil, at the surface of the soil constrains most of the waves to propagate within the soil layer below the pavement. The pavement itself carries part of the energy of the waves but at a different velocity than those travelling through the soil. In Figure 2A and 2A1, most of the energy of the wavefield has not yet reach the structure and its energy is concentrated at the surface of the model. As the wavefield reaches the concrete structure in Figure 2B and 2B1, part of its energy is scattered toward to the surface while the rest of the wavefield starts to travel along the roof and the wall of the structure. The part of the wavefield that travels between the roof of the concrete structure and the surface of the soil or the pavement is trapped within this zone that acts as a waveguide. Multiple reflections then occur within the waveguide (Figure 2C1). Figure 2D shows how the manhole reflects part of the wavefield as it reaches it.

Figure 4 shows all the recorded signals (accelerograms) along line 3 in the form of a contour plot where the amplitude of every signal was normalized with respect to the maximum absolute amplitude recorded by each signal. The normalization process is necessary in order to view all the signals since their amplitude decays as the waves move away from the source due mainly to geometrical spreading. Although the geometrical spreading of Rayleigh waves can be predicted and corrected when they travel through a normally dispersive media, this correction is not trivial when they travel through other media. The normalization process, however, causes the loss of some of the information that could be retrieved from the changes in amplitudes of the different waves travelling through the models. Nevertheless, this aspect was chosen not to be discussed in this study.

The effect of the pavement, the concrete structure and of the multiple reflections occurring within the waveguide

are all visible on the accelerograms recorded at the surface of the models (Figure 4). First, prior to the beginning of the structure at 1.0 m, most of the energy carried by the waveform travels at the same velocity. Near the beginning of the structure at a distance of 1.0 m from the source, the shape of the waveform after 0.01 second changes and the energy is no longer travelling at the same velocity. The change in shape is due to the waves that are reflected by the beginning of the concrete structure. Second, the multiple reflections caused by the presence of the pavement and the structure can be identified as late arrivals on the recorded signals as shown in Figure 4. Finally, as the elastic waves travel within the waveguide between 1.0 and 3.0 m, the changes into the shape of the waveform between 0.01 and 0.02 s are due to the coupling and uncoupling of the different waves travelling through the waveguide at different velocities and amplitudes.

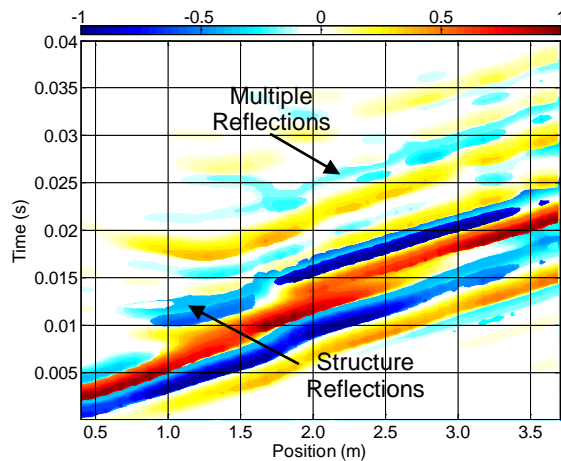


Figure 4. Vertical acceleration recorded by the receivers positioned along line 3.

5 EFFECT OF THE MANHOLE

The presence of the manhole linking the concrete structure to the surface of the soil causes the reflection of part of the elastic waves reaching it. Figure 5a shows the vertical acceleration recorded at the surface of model 1 which only contains a concrete structure surrounded by soil while Figure 5b shows the same profile but for the model 2 which contains a manhole. No pavement is present at the surface of both models. On Figure 5b, the elastic waves that are reflected from the manhole are visible as the waveform propagating at a different rate than the non-reflected waves travelling from the source. In Figure 5b, at a position of 1.0 m, the time delay between the arrival of the waves travelling along the surface of the structure and the arrival of the waves reflected from the manhole is 0.015 s. However, at a position of 2.5 m, the arrival times of the direct and the reflected waves are similar and they can no longer be separated by visually looking at the traces. To verify how the reflected waves affect the recorded signals, the group velocities are calculated at 2 different positions, 1.0 and 2.5 m, for both models (Figure 6). On the group velocity profiles

calculated at a position of 1.0 m in Figure 6b, the effect of the manhole is characterized by the presence, between 100 and 400 Hz, of energy travelling at a constant velocity of 55 m/s. Below 100 Hz, the effect of the presence of the manhole is negligible as the group velocities of both models are the same. At a position of 2.5 m (Figure 6d), the reflected waves merge with the other waves and the group velocity calculated between 80 and 250 Hz appears to be higher in the model where the manhole is present. The effect of the manhole on the group velocity is mainly controlled by the amount of energy carried by the reflected waves. This amount of energy is controlled by the 'reflectivity' of the manhole and the distance between a receiver and the manhole. The presence of the manhole should, therefore, be accounted for in the analysis of the results. However, although it will not be shown in this paper, the presence of a pavement at the surface of the soil significantly reduces the effect of the manhole on the recorded acceleration.

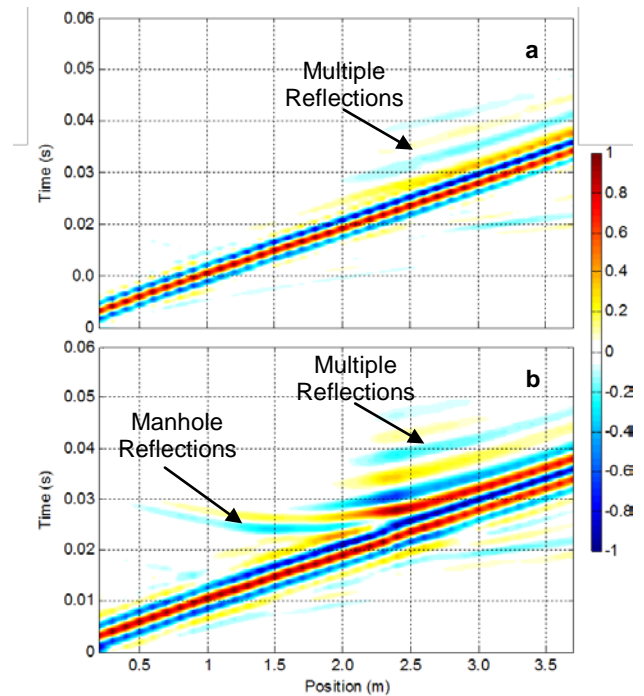


Figure 5. Vertical acceleration recorded for line 1 (model1) and line 2 (model 2).

6 GROUP VELOCITY PROFILES

The procedure followed to detect the presence of discontinuities at the surface of the roof of an underground structure based on the energy, the group velocity and the phase velocity of surface waves was presented in Tremblay et al. (2014). In this study, only the group velocity profiles, calculated with reference from the location of the source (0 m), of the different lines are presented. These group velocity profiles will be used to show how the location of the line with respect to the position of the edges of the structure and with respect to the position of a discontinuity influences the recorded velocities. To account for the location of the line with

respect to the edges of the structure, 2 lines (lines 3 and 4) are performed over the same underground structure (model 3) but at a different location with respect to the edge of the underground structure as shown in Figure 3. The effect of the presence of a damaged zone at the surface of the concrete structure will be studied with the line 5 performed directly over the damaged zone and with the line 6 performed near the edge of the structure of model 4.

6.1 Effect of the edges and the discontinuity

As elastic waves propagate through the different models, their group velocity changes due to the presence of the concrete structure which reflects part of the energy of the waves travelling from the source as shown in Figure 2. For the receivers placed near the location of the beginning of the concrete structure at 1.0 m, the recorded wavefield consists mainly of the wavefield travelling directly from the source and the wavefield reflected from the edge of the structure.

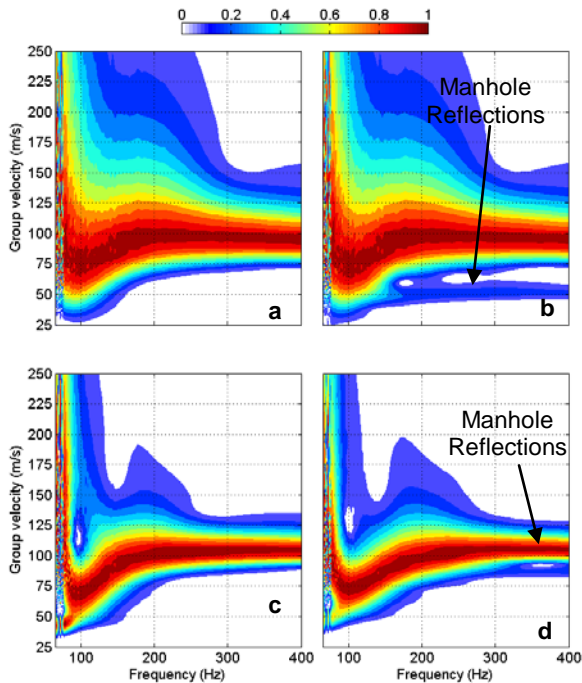


Figure 6. Vertical acceleration recorded at different positions: a) Line 3, position 1.0 m. b) Line 4, position 1.0 m. c) Line 3, position 2.5 m. d) Line 4, position 2.5 m.

The group velocity profiles of Fig 7 and 8 are therefore an average of the group velocities of both wavefields. Since the group velocities of the reflected waves are lower at greater distances from the structure, the group velocities measured prior to the beginning of the structure increases rapidly as we approach the position of the beginning of the structure. However, at a certain distance passed the beginning of the structure, the group velocity sharply decreases due to the arrival of the multiple reflections caused by the presence of the concrete structure. Near the end of the concrete structure at a position of 3.0 m, the group velocity tends to decrease because the elastic

waves are no longer confined to the shallow soil layer above the concrete structure and below the pavement.

The group velocity profiles shown in Figure 6 demonstrate the relationship between the frequency (wavelength) and the group velocity. The presence of a minimum value at 100 Hz in the group velocity profiles of Figure 6 is characteristic of the presence of the concrete structure. It is therefore expected that the group velocity will vary depending on the frequency at which it is calculated.

Figure 7 shows the group velocity profile calculated at 85 and 100 Hz for lines 3 and 4 performed over the structure of model 3. As shown in Figure 7, the group velocities measured over the structure between 1.0 and 3.0 m are lower when measured near the edges of the structure in line 4.

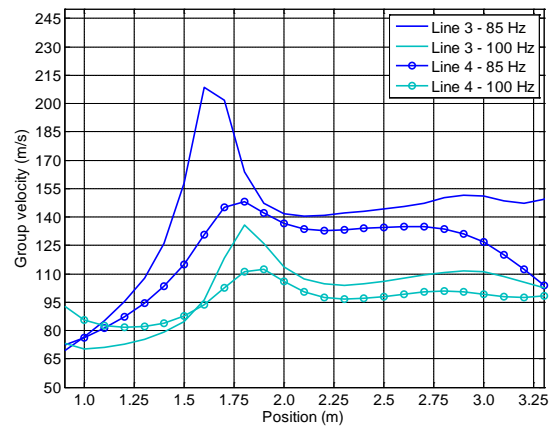


Figure 7. Group velocity profiles of lines 3 and 4 at 85 and 100 Hz.

This is because near the edges of the structure, a larger proportion of the energy carried by the waves will leak through the sides of the structure which no longer acts as a waveguide for these waves. The group velocities are also higher at 85 Hz than at 100 Hz due to the important variation of the group velocity near 100 Hz (Figure 6). The group velocities of line 3 are however higher than the group velocities of line 4 before 1.0 m at 85 Hz and before 1.5 m at 100 Hz. This can be explained by the presence of the waves that are reflected by the structure and that are causing an apparent decrease of the group velocity until they are fully coupled with the main wavefield. For the line 4 located near the edge of the structure, the amount of energy reflected by the structure is lower meaning that the reflected waves will have a smaller impact of the overall group velocity than for line 3.

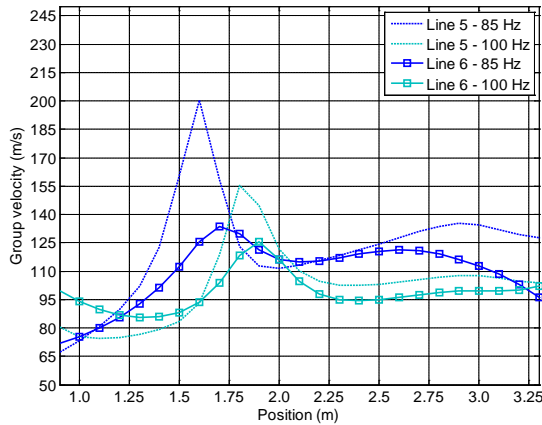


Figure 8. Group velocity profiles of lines 5 and 6 at 85 and 100 Hz

Figure 8 presents the group velocity recorded for the lines 5 and 6 performed over a concrete structure with a damaged roof. As mention in section 3.1, the discontinuity consists of a zone of lower velocity and varying depth located at the surface of the roof of the concrete structure as indicated by the dashed rectangular zones in Fig 9c-d.

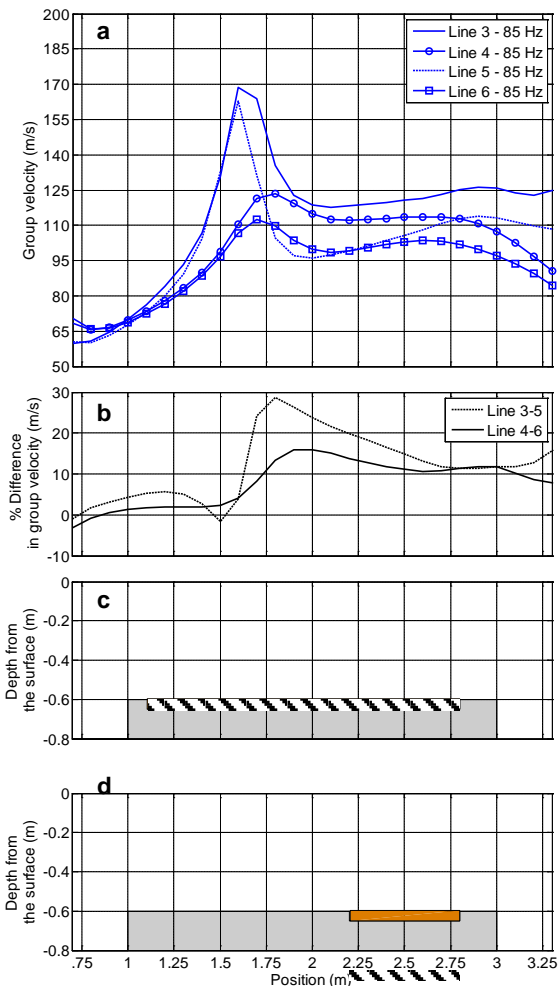


Figure 9. a: Group velocities measured over the models 3 and 4. b: Difference in % between the group velocity of lines 3 and 5 and of line 4 and 6. c: Location of the surface of the concrete structure and of the damaged zone under the lines 3-5 along the X-axis. D: Location of the surface of the concrete structure and of the damaged zone under the lines 4-6 along the X-axis

Figure 8 shows the group velocity of the waves propagating at a frequency 85 and 100 Hz measured along the lines 5 and 6 of model 4. At 85 Hz, the group velocities measured near the edge of the structure (line 6) are higher than the group velocities measured farther from the edge (line 5) due to the presence of the damaged zone at the surface of the structure. The comparison of the group velocities measured over model 3 with the ones measured over model 4 suggests that the waves propagating at 85 are affected more by the presence of the discontinuity than the waves propagating at 100 Hz. Figure 9a shows the difference between the group velocities recorded over model 3 and model 4 at 85 Hz. The difference in percentages between the lines 3-5 and the lines 4-6 are shown in Figure 9b while the Figure 9c-d show the position of the structure and of the damaged zone. The presence of the damaged zone causes a maximum variation of the group velocity of 29 % for the lines 3-5 and of 16 % for the lines 4-6. The higher variation of the group velocities between the line 3 and the line 5 is due to the size of the damaged zone below these 2 lines.

7 CONCLUSIONS

The inspection of underground structures is often a non-trivial task due to their limited accessibility. For these types of structures, non-destructive techniques are particularly suitable. In the past decade, NDTs based on the propagation of surface waves have been successfully used for different types of underground surveys. In this study, 3-dimensional models were used to show how the propagation of surface waves is affected by the presence and configuration of an underground concrete structure. The propagation of surface waves in a medium where the elastic properties may vary in all directions is analytically difficult to solve. Numerical methods are most suitable for these types of problems. FLAD3D, a 3-dimensional finite difference software was used to model the propagation of surface waves. Three-dimensional models were first used to study how the propagation of surface waves is affected by the presence of a manhole linking the structure to the surface of the soil. The presence of the manhole was shown to increase or decrease the group velocity recorded at a given location depending on the frequency at which it is calculated. It was also shown how the presence of a pavement at the surface of the soil profile affects the propagation of surface waves. Finally, this article shows that the group velocity of surface waves travelling through a model containing a concrete structure is affected by the condition of the surface of the roof of the structure.

ACKNOWLEDGEMENTS

The authors would like to thank Hydro-Québec and the NSERC for their financial support throughout this research project.

REFERENCES

- Aki, K. and Richard, P.G. 2002. *Quantitative Seismology*. University Science Books, Sausalito, CA
- Fichtner, A. 2011. *Full Seismic Waveform Modelling and Inversion*. AGEM. Springer-Verlag Berlin Heidelberg
- Gabriels, P., R. Snieder, and G. Nolet., 1987, In situ measurements of shear wave velocity in sediments with higher-mode Rayleigh waves: *Geophysical Prospecting*, **35**, 187–196.
- Itasca. 2014. *FLAC: fast lagrangian analysis of continua users guide*. Minneapolis, MN: Itasca consulting group Inc.
- Jones, R. 1962. Surface wave techniques for measuring elastic properties and thickness of roads: Theoretical development. *British Journal of Applied Physics*, **13**: 21–29
- Karray, M. 1999. *Utilisation de l'analyse modale des ondes de Rayleigh comme outil d'investigation géotechnique in-situ*, Thèse de doctorat en génie civil, Département de génie civil, Université de Sherbrooke, Sherbrooke (Québec), Canada, 275p.
- Karray, M. and Lefebvre, G. 2009. Detection of cavities beneath pavements by modal analysis of surface waves (Rayleigh waves) (MASW). *Canadian Geotechnical Journal*, 46 (4), pp. 424-437.
- Karray, M., Lefebvre, G., Ethier, Y. et Bigras, A. (2010). Assessment of deep compaction of the peribonka dam foundation using "modal analysis of surface waves" (MASW). *Canadian Geotechnical Journal*, volume 47, numéro 3, p. 312-326.
- Kennett, B.L.N. 1979. Seismic waves in a stratified half space. *Geophys. J.R. Astron. Soc.* **57**, 557-583
- Kuhlemeyer, R. L., and Lysmer, J. 1973. Finite Element Method Accuracy for Wave Propagation Problems. *J. Soil Mech. & Foundations, Div. ASCE*, 99(SM5), 421-427
- Lamb, H. 1904. On the propagation of tremors over the surface of an elastic solid. *Philos. Trans. R. Soc. Lond.* A203. 1-42
- Lysmer, J., Kuhlemeyer, R.L. 1969. Finite dynamic model for infinite media. *J Eng Mech Div* ;95:859–77.
- Nazarian, S., 1984, In situ determination of elastic moduli of soil deposits and pavement systems by spectral-analysis-of-surface waves method: Ph.D. dissertation, University of Texas at Austin.
- Park, C.B., Miller, R.D., Xia, J., 1999. Detection of near-surface voids using surface waves. *SAGEEP 99*, Oakland, Calif., pp. 281 – 286.
- Schwab, F.A., Knopoff, L., 1972. Fast Surface Wave and Free Mode Computations: in *Methods in Computational Physics*. In: Bolt, B.A. (Ed.), Academic Press, New York, pp. 87–180.
- Socco, L.V., Foti, S., Boiero, D., 2010. Surface wave analysis for building near surface velocity models: established approaches and new perspectives. *Geophysics SEG*, 75:A83–A102
- Tremblay, S.P., Karray, M., Chekired, M., Bessette, C., Jinga, L. 2014. Non-destructive inspection of the surface of underground structures based on the propagation of surface waves *GeoRegina 2014*, 67^e conférence géotechnique canadienne, Regina, Sask.